Theory of electron spin decoherence by interacting nuclear spins in a quantum dot

Wang Yao,[1,*] Ren-Bao Liu,[1,2] and L. J. Sham[1]
[1]*Department of Physics, University of California San Diego, La Jolla, California 92093-0319, USA*
[2]*Department of Physics, The Chinese University of Hong Kong, Shatin, N.T., Hong Kong, China*
(Received 11 May 2006; revised manuscript received 1 August 2006; published 1 November 2006)

We present a quantum solution to the electron spin decoherence by a nuclear pair-correlation method for the electron-nuclear spin dynamics under a strong magnetic field and a temperature high for the nuclear spins but low for the electron. The theory incorporates the hyperfine interaction, the intrinsic (both direct and indirect) nuclear interactions, and the extrinsic nuclear coupling mediated by the hyperfine interaction with the single electron in question. The last is shown to be important in free-induction decay (FID) of the single electron spin coherence. The spin-echo eliminates the hyperfine-mediated decoherence but only reduces the decoherence by the intrinsic nuclear interactions. Thus, the decoherence times for single spin FID and ensemble spin-echo are significantly different. The decoherence is explained in terms of quantum entanglement, which involves more than the spectral diffusion.

DOI: 10.1103/PhysRevB.74.195301 PACS number(s): 03.65.Yz, 76.60.Lz, 76.70.Dx, 73.21.La

I. INTRODUCTION

Irreversible processes of a microscopic system in contact with a macroscopic system are central to nanoscience and to quantum information science. A canonical example is the spin decoherence and relaxation of an electron localized by an impurity, an electrical gate, or a quantum dot in a semiconductor, which have been extensively studied both in theory[1–12] and in experiments.[13–20] Single dot spin relaxation time $T_1 \gtrsim 0.1$ ms has been measured for different quantum dot systems at low temperature,[13–16] in good agreement with theoretical estimates.[9,10] The single spin decoherence time T_2 has a lower bound of 10 ns established by the measurements of the inhomogeneously broadened T_2^* for either a spatial ensemble of many dots[17] or a time ensemble of a single dot.[18–20] Spin dephasing by phonon scattering in quantum dots is suppressed at temperature below a few Kelvins,[8,11] leaving the nuclear spins as the dominant mechanism for electron spin dephasing. References 4 and 5 gave, respectively, a theory and a numerical study of the effects of off-diagonal electron nuclear hyperfine interaction. References 6, 7, and 21 gave treatments of the effects of nuclear dipolar interaction and calculated the electron spin decoherence time with an ensemble spin-echo.

Our pursuit of a quantum theory of decoherence without the restriction of a stochastic theory[1,6] is motivated by the need to control the electron spin decoherence. The nuclear spins coupled to the electron by the hyperfine interaction are taken to be the sole source of decoherence as in Refs. 2 and 4. However, we treat the interaction between nuclear spins which will be shown to be important in the high magnetic field regime while the neglect of the nuclear spin interaction in Refs. 2 and 4 is valid in the low field regime. Our method of solution of the many-spin problem keys on the evolution of the two flip-flop states of each pair of nuclear spins and is thus termed the pseudospin method. We establish conditions for the validity of our method. The method is simple enough for many applications, including the more advanced design of pulse control of the electron spin to eliminate the decoherence effects.[22] It also produces a simple physical picture, which greatly aids the applications. We divide the interaction between two nuclear spins into two types, intrinsic and extrinsic, respectively independent and dependent on the single electron spin state. The intrinsic interaction consists of the dipole-dipole coupling and the indirect coupling mediated by virtual interband spin transitions via the hyperfine interaction.[23–27] The extrinsic nuclear interaction is mediated by virtual spin flips between each of the two nuclei and the single electron due to the off-diagonal hyperfine coupling.

The results presented here are (i) a basic solution of the decoherence dynamics, both for a single electron spin and for an ensemble of independent electrons; (ii) numerical evaluations for GaAs dots; and (iii) an analysis of the different time dependence of coherence for intrinsic and extrinsic nuclear-nuclear interaction. We will show that the extrinsic hyperfine-mediated nuclear interaction plays an important role in single spin FID. The spin-echo not only refocuses the dephasing by inhomogeneous broadening in ensemble dynamics but also eliminates the decoherence by extrinsic hyperfine-mediated nuclear interaction. Thus, the decoherence times for single spin FID and spin-echo are significantly different. The usual practice of inferring the single electron spin dephasing time from ensemble echo measurement could be problematic. Note that in NMR literature, the difference in time scale of FID and echoes, when the inhomogeneous effect is excluded, was first recognized.[28–30]

The electron spin decoherence arises out of quantum entanglement between the electron spin states $|\pm\rangle$ and the many-nuclear spin states $|\mathcal{J}\rangle$. When a coherent electron spin state $C_+|+\rangle+C_-|-\rangle$ is prepared, the initial state of the whole electron-nuclear system is the product state, $(C_+|+\rangle+C_-|-\rangle)\otimes|\mathcal{J}\rangle$. In time t, the nuclear states associated with the two electron spin states diverge, yielding an entangled state of the form, $C_+|+\rangle\otimes|\mathcal{J}^+(t)\rangle+C_-|-\rangle\otimes|\mathcal{J}^-(t)\rangle$. The electron spin coherence is measured by $|\langle\mathcal{J}^-(t)|\mathcal{J}^+(t)\rangle|$ when the nuclear spin degrees of freedom are traced out. Our theory consists in a direct attack of the many nuclear spin dynamics. The assumption of the pure electron spin decoherence time T_2 being much shorter than its longitudinal spin relaxation time T_1 will be shown to lead to a simple effective Hamiltonian for

the whole system of the form $\Sigma_{\pm}|\pm\rangle\hat{H}_{\pm}\langle\pm|$ in terms of the nuclear spin Hamiltonians $\hat{H}_{\pm}$. This simplifies the electron spin coherence to the overlap of the two nuclear spin states, each following the evolution conditioned on one spin state of the electron, $|\langle\mathcal{J}|e^{i\hat{H}_-t}e^{-i\hat{H}_+t}|\mathcal{J}\rangle|$.

This entanglement approach to decoherence has an interesting relation to the antecedents in the decoherence literature. The square of the decoherence is formally the same as the Loschmidt echo if $\hat{H}_-$, say, is regarded as $\hat{H}_+$ with a perturbation, which is related to the decoherence of the nuclear spin system.[31,32] A model of a single spin coupled to a transverse field Ising chain is used to study the effect of quantum phase transition on the decoherence of the Ising chain.[33] A key change in the model could make it a study of the decoherence of the single spin in the Ising spin bath.

We will show that the nuclear spin dynamics is dominated by the nuclear spin pair-flips. The pairs can be treated as independent of one another and only the two-spin correlations need be taken into account in the interacting nuclear spin dynamics. On a time scale small compared with the inverse nuclear couplings but ample for the electron spin decoherence, the number of pair-flip excitations are small compared with the number of nuclear spin pairs available for spin-flip, which come from the randomization of the nuclear spin directions at a temperature higher than the nuclear spin temperature, i.e., 10 mK$\lesssim T\lesssim$1 K (still low enough to avoid the effects of the electron-phonon scattering). The cluster expansion by Witzel *et al.*[7] yields an equivalent pair-correlation approximation. We will establish the pseudospin model in which the elementary excitations by independent pair-flips are just rotations of noninteracting 1/2 spins.

Numerical evaluations for a GaAs dot then require no further approximation. The electron spin decoherence is calculated for a range of magnetic field strength (1–40 T) and various dot sizes. The pseudospin rotation yields the following analysis of the results. The e^{-t^n} short-time behavior obeys $n=2$ or 4 depending on the dominance of, respectively, the extrinsic and the intrinsic nuclear-nuclear interaction. In the long time limit, the crossover to the exponential decay ($n=1$) indicates the onset of the Markovian kinetics.

The main body of the text gives a succinct account of the key points of the theory and the results of the computation. Section II defines the single electron system coupled to a bath of interacting nuclear spins. Section III defines the electron spin coherence and formulates the quantum theory of its evolution. Section IV describes the pseudospin solution. Section V gives an evaluation of the decoherence for a GaAs quantum dot. Section VI serves as a brief summary of the main results. So as not to interrupt the flow of the essence of simple exposition of our decoherence theory, further details of the theory are grouped in the Appendixes.

II. SINGLE ELECTRON IN INTERACTING NUCLEAR SPIN BATH

The system consists of an electron with spin vector $\hat{\mathbf{S}}_\mathbf{e}$ and N nuclear spins, $\hat{\mathbf{J}}_n$, with Zeeman energies Ω_e and ω_n under a magnetic field B_{ext}, respectively, where n denotes both positions and isotope types (e.g., ^{75}As, ^{69}Ga, and ^{71}Ga in GaAs). The Hamiltonian of this system is described in Appendix A. The interaction can be separated as "diagonal" terms which involve only the spin vector components along the field (z) direction and "off-diagonal" terms which involve spin-flips (see Appendix B). Because the electron Zeeman energy is much larger than the strength of the hyperfine interaction, the off-diagonal term is eliminated by a standard canonical transformation, with the second-order correction left as the hyperfine-mediated nuclear interaction. For the same reason, the off-diagonal part of the nuclear interaction contributes only when the terms conserve the Zeeman energies (so-called secular terms in the NMR terminology). Hence, the nonsecular terms are negligible. The total reduced Hamiltonian is obtained from the transformation in Appendix B, for the limit of long longitudinal relaxation time ($T_1\to\infty$),

$$\hat{H}_{\text{red}}=\hat{H}_e+\hat{H}_N+\sum_{\pm}|\pm\rangle\hat{H}_{\pm}\langle\pm|, \tag{1}$$

with $\hat{H}_e=\Omega_e\hat{S}_e^z$, $\hat{H}_N=\omega_n\hat{J}_n^z$, and the interaction terms,

$$\hat{H}_{\pm}=\pm\hat{H}_A+\hat{H}_B+\hat{H}_D\pm\hat{H}_E, \tag{2}$$

given by

$$\hat{H}_A=\sum_{n\neq m}{}'\frac{a_n a_m}{4\Omega_e}\hat{J}_n^+\hat{J}_m^-\equiv\sum_{n\neq m}{}'A_{n,m}\hat{J}_n^+\hat{J}_m^-, \tag{3a}$$

$$\hat{H}_B=\sum_{n\neq m}{}'B_{n,m}\hat{J}_n^+\hat{J}_m^-, \tag{3b}$$

$$\hat{H}_D=\sum_{n<m}D_{n,m}\hat{J}_n^z\hat{J}_m^z, \tag{3c}$$

$$\hat{H}_E=\sum_n\frac{a_n}{2}\hat{J}_n^z\equiv\sum_n E_n\hat{J}_n^z, \tag{3d}$$

where $|\pm\rangle$ are the eigenstates of $\hat{S}_\text{e}^z$, the summation with a prime runs over only the homonuclear pairs, the subscript A denotes the extrinsic hyperfine mediated interaction, B the off-diagonal part of the intrinsic interaction, D the diagonal part of the intrinsic interaction, and E the diagonal part of the contact electron-nuclear hyperfine interaction. The hyperfine energy,[34] determined by the electron wave function, has a typical energy scale $E_n\sim a_n\sim 10^6$ s^{-1} for a dot with about 10^6 nuclei. The sum, $\mathcal{A}\equiv\Sigma_n a_n$, is the *hyperfine constant* depending only on the material. The intrinsic nuclear spin-spin interaction has the near-neighbor coupling $B_{n,m}\sim D_{n,m}\sim 10^2$ s^{-1}. The hyperfine mediated interaction, which is unrestricted in range and associated with opposite signs for opposite electron spin states, has an energy scale dependent on the field strength, $A_{n,m}\sim 1-10$ s^{-1} for field $\sim$40–1 T.

III. DECOHERENCE THEORY

The electron-nuclear spin system is assumed to be initially prepared in a product state with the nuclear spins in a

thermal state with temperature T, described by the density matrix

$$\hat{\rho}(0) = \hat{\rho}^e(0) \otimes \hat{\rho}^N. \tag{4}$$

The time evolution of the reduced density matrix of the electron spin,

$$\hat{\rho}^e(t) = \mathrm{Tr}_N\, \hat{\rho}(t), \tag{5}$$

obtained by tracing over the nuclear spins, may be expressed in the form

$$\rho^e_{\mu,\nu}(t) = \sum_{\mu',\nu'} \mathcal{L}_{\mu,\nu;\mu',\nu'}(t)\rho^e_{\mu',\nu'}(0), \tag{6}$$

where $\rho^e_{\mu,\nu} \equiv \langle\mu|\rho^e|\nu\rangle$, and $|\mu\rangle$, $|\nu\rangle \in \{|+\rangle, |-\rangle\}$. The superoperator or correlation function $\mathcal{L}_{\mu,\nu;\mu',\nu'}$ can be expressed in terms of the evolution operator and contains the information on the electron spin relaxation and decoherence.

The Hamiltonians of Eq. (1) for the $T_1 \to \infty$ limit conserves the electron $\hat{S}^z_e$ quantum number, $[\hat{H}, \hat{S}^z_e] = 0$. Hence, the correlation function has the following properties:

$$\mathcal{L}_{\mu,\nu;\mu',\nu'}(t) = \mathcal{L}_{\mu,\nu}(t)\delta_{\mu,\mu'}\delta_{\nu,\nu'}, \tag{7a}$$

$$\mathcal{L}_{\mu,\mu}(t) = 1, \tag{7b}$$

$$\mathcal{L}_{+,-}(t) = \mathcal{L}^*_{-,+}(t), \tag{7c}$$

and the specific expression for the free-induction decay,

$$\mathcal{L}_{+,-}(t) = e^{-i\Omega_e t}\mathrm{Tr}_N(\hat{\rho}^N e^{+i\hat{H}_- t} e^{-i\hat{H}_+ t}), \tag{8}$$

which can be straightforwardly extended to dynamics under pulse control.

The ensemble of nuclear spins, at temperature $T \gtrsim \omega_n \gg A_{n,m}, B_{n,m}, D_{n,m}, E_n$, may be approximated by the density matrix,

$$\hat{\rho}^N \approx e^{-\hat{H}_N/T} = \sum_{\mathcal{J}} P_{\mathcal{J}} |\mathcal{J}\rangle\langle\mathcal{J}|, \tag{9}$$

where $|\mathcal{J}\rangle \equiv \otimes_n |j_n\rangle$, j_n being the quantum number of nuclear spin n in the magnetic field direction. $P_{\mathcal{J}}$ is the thermal distribution factor. The correlation function $\mathcal{L}_{+,-}(t)$ can then be generally expressed as

$$\mathcal{L}_{+,-}(t) = \sum_{\mathcal{J}} P_{\mathcal{J}} e^{-i\phi_{\mathcal{J}}(t)} |\langle\mathcal{J}^-(t)|\mathcal{J}^+(t)\rangle|. \tag{10}$$

In FID, $|\mathcal{J}^\pm(t)\rangle = e^{-i\hat{H}^\pm t}|\mathcal{J}\rangle$ and $\phi_{\mathcal{J}}(t) = (\Omega_e + \mathcal{E}_{\mathcal{J}})t$ where $\mathcal{E}_{\mathcal{J}} = \Sigma_n j_n a_n$ is the contribution to the electron Zeeman splitting from the Overhauser field in the nuclear configuration $|\mathcal{J}\rangle$. With a π pulse to flip the electron spin at time τ, we have $|\mathcal{J}^\pm(t > \tau)\rangle = e^{-i\hat{H}^\mp(t-\tau)} e^{-i\hat{H}^\pm \tau}|\mathcal{J}\rangle$ and $\phi_{\mathcal{J}}(t > \tau) = (\Omega_e + \mathcal{E}_{\mathcal{J}})(2\tau - t)$.

An important finding is that the coherence for the ensemble dynamics takes the factored form

$$\mathcal{L}_{+,-}(t) = \mathcal{L}^s_{+,-}(t) \times \mathcal{L}^{(0)}_{+,-}(t), \tag{11}$$

where

$$\mathcal{L}^s_{+,-}(t) = |\langle\mathcal{J}^-(t)|\mathcal{J}^+(t)\rangle|, \tag{12a}$$

$$\mathcal{L}^{(0)}_{+,-}(t) = \sum_{\mathcal{J}} P_{\mathcal{J}} e^{-i\phi_{\mathcal{J}}(t)}. \tag{12b}$$

$\mathcal{L}^s_{+,-}(t)$ characterize the electron coherence evolution in the *single-system dynamics* with the nuclear bath begins on a typical pure initial state $|\mathcal{J}\rangle \equiv \otimes_n |j_n\rangle$. The single-system dynamics is solely determined by the spectrum of the elementary excitations from the initial state $|\mathcal{J}\rangle$, i.e., the nuclear spin pair-flips driven by $\hat{H}_A$ and $\hat{H}_B$ in Eqs. (3a) and (3b). For a sufficiently large number N of the nuclear spins, the spectrum is independent of the initial state with an error of the order of $1/\sqrt{N}$. Therefore the coherence factor $\mathcal{L}^s_{+,-}(t)$ can be pulled out of the sum over $\mathcal{J}$ which results in the factorized form as in Eq. (11). The independence of the nuclear pair excitation spectrum on the initial state has been numerically verified with a number of different initial states in a GaAs quantum dot with $N = 10^6$. The independence of $\mathcal{L}^s_{+,-}(t)$ on the initial nuclear state $|\mathcal{J}\rangle$ makes the measurement of single-system coherence possible in principle, e.g., in single spin measurement with predetermination or post-selection of local Overhauser field through projective measurement.[4]

The ensemble effect resides entirely in the factor $\mathcal{L}^{(0)}_{+,-}(t)$, which may be read as the inhomogeneous broadening of the local field $\mathcal{E}_{\mathcal{J}}$ with distribution function $P_{\mathcal{J}}$. The inhomogeneous factor (i.e., the distribution of the hyperfine energy $\mathcal{E}_{\mathcal{J}}$) dominates the free induction decay in the ensemble dynamics in the form of $\mathcal{L}^{(0)}_{+,-}(t) = e^{-i\Omega_e t - (t/T_2^*)^2}$, with the dephasing time $T_2^* \sim \sqrt{N}\mathcal{A}^{-1} \sim 10$ ns as measured.[17–20] To single out the dynamical decoherence time from the T_2^*, spin-echo pulses can be applied to eliminate the effects of the static fluctuations of the local field. After a π pulse applied at τ, the inhomogeneous broadening part of the correlation function $\mathcal{L}^{(0)}_{+,-}(t) = 1$ for $t = 2\tau$. The ensemble coherence peak at 2τ is known as spin-echo.[35] The spin-echo profile, i.e., the echo magnitude $\mathcal{L}_{+,-}(2\tau) = \mathcal{L}^s_{+,-}(2\tau)$ plotted as a function of the echo delay time 2τ, reveals the dynamical processes that leads to decoherence.

IV. THE PSEUDOSPIN SOLUTION

The solution to the single-system evolution $|\mathcal{J}^\pm(t)\rangle$ relies on the pair-correlation approximation explained here with more details in Appendix C and justified in Appendix D. Within a time t much smaller than the inverse nuclear interaction strength, the total number of pair-flip excitations N_{flip} is much smaller than the number of nuclei N. The probability of having pair-flips correlated is estimated in Appendix C 3 to be $P_{\mathrm{corr}} \sim 1 - e^{-qN^2_{\mathrm{flip}}/N}$ (q being the number of homonuclear nearest neighbors), which, as also shown by *a posteriori* numerical check, is well bounded by $\sim 1\%$ in the worst scenario studied in this paper. Thus, the pair-flips as elementary excitations from the initial state can be treated as independent of each other, with a relative error $\epsilon \lesssim P_{\mathrm{corr}}$. Then the single-system dynamics $|\mathcal{J}^\pm(t)\rangle$ can be described by the excitation of pair correlations as noninteracting quasiparticles from the "vacuum" state $|\mathcal{J}\rangle$, driven by the "low-energy" effective Hamiltonian,

$$\hat{H}^{\pm}_{\mathcal{J}} = \sum_k \hat{\mathcal{H}}^{\pm}_k \equiv \sum_k \mathbf{h}^{\pm}_k \cdot \hat{\boldsymbol{\sigma}}_k/2, \tag{13}$$

which has been written in such a way that the pair correlations are interpreted as 1/2-pseudospins, represented by the Pauli matrix $\hat{\boldsymbol{\sigma}}_k$, with k labelling all possible pair-flips, defined in more details in Appendix C 4. The time evolution from the initial state $|\mathcal{J}\rangle$ can be viewed as the rotation of the pseudospins, initially all polarized along the $+z$ pseudoaxis: $\otimes_k|\uparrow_k\rangle$, under the effective pseudomagnetic field,

$$\mathbf{h}^{\pm}_k \equiv (\pm 2A_k + 2B_k, 0, D_k \pm E_k), \tag{14}$$

where, for the electron spin state $|\pm\rangle$, $\pm A_k$ and B_k are the pair-flip transition amplitudes, defined in Eqs. (C2), contributed by the hyperfine mediated coupling $\hat{H}_A$ and the intrinsic coupling $\hat{H}_B$, respectively, and D_k and $\pm E_k$ are the energy cost of the pair-flip contributed by the diagonal nuclear coupling $\hat{H}_D$ and the hyperfine interaction $\hat{H}_E$, respectively. The decoherence then can be analytically derived as

$$\mathcal{L}^s_{+,-}(t) = \prod_k |\langle \psi^-_k | \psi^+_k \rangle| \approx \prod_k e^{-\delta_k^2/2}, \tag{15}$$

where $|\psi^{\pm}_k\rangle$ are the conjugate pseudospin states. In FID, $|\psi^{\pm}_k(t)\rangle \equiv e^{-i\hat{\mathcal{H}}^{\pm}_k t}|\uparrow_k\rangle$; while with a π pulse to flip the electron at $t=\tau$, $|\psi^{\pm}_k(t>\tau)\rangle \equiv e^{-i\hat{\mathcal{H}}^{\mp}_k (t-\tau)} e^{-i\hat{\mathcal{H}}^{\pm}_k \tau}|\uparrow_k\rangle$. $\delta_k^2 \equiv 1 - |\langle \psi^-_k | \psi^+_k \rangle|^2$ possesses a simple geometrical interpretation: the squared distance between the two conjugate pseudospins on the Bloch sphere, which quantifies the entanglement between the electron spin and the pseudospins.

V. RESULTS OF DECOHERENCE AND SPIN-ECHO FOR A QUANTUM DOT

In this section, we analyze the results of decoherence under free induction and spin-echo conditions for a GaAs quantum dot. In numerical evaluations, the GaAs dot is assumed to have a hard-wall confinement in the growth direction [001] with thickness $L_{[001]}$ and a parabolic confinement with Fock-Darwin radius r_0 in the lateral directions. The external magnetic field is applied along the [110] direction. For the indirect intrinsic nuclear interaction, we consider only the exchange part.[27] The g factor of the electron[17] is taken as −0.13. The initial state $|\mathcal{J}\rangle$ is generated by randomly setting each nuclear spin according to a "high-temperature" Boltzmann distribution ($P_{\mathcal{J}}$=constant).

Figure 1 shows the FID in single-system dynamics for a typical dot under various field strengths B_{ext}. The inset of Fig. 1 shows the field dependence of decoherence time T_2 which is defined as the time when the FID signal is $1/e$ of its initial value. The strong field dependence of T_2 demonstrate the significance of the extrinsic hyperfine mediated nuclear coupling until it is suppressed by a very strong field (~20 T). As shown in Fig. 1, the FID signals have significantly different decoherence times from the spin-echo signals (see also Fig. 4). In Fig. 2, we separate artificially the contributions from the extrinsic hyperfine-mediated and the intrinsic nuclear interactions and show their different dependence on time and dot size. The spin-echo profile is also plotted for comparison.

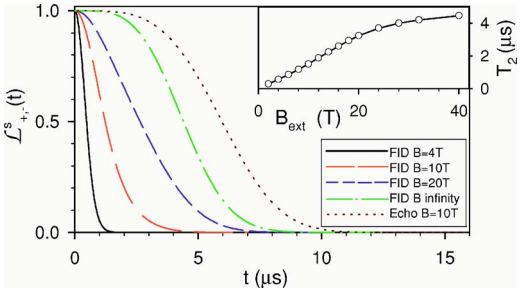

FIG. 1. (Color online) Single-system FID for a dot with $L_{[001]}$ =2.8 nm and r_0=15 nm under various field strengths. The spin-echo profile as a function of $t=2\tau$ for B_{ext}=10 T is also plotted for comparison. The insets show the field dependence of the FID decoherence time.

A couple of justified simplifications can provide an understanding of the effects of various mechanisms on the spin decoherence. First, the energy cost by the diagonal nuclear coupling (D_k) can be neglected as it is by three orders of magnitude smaller than that by hyperfine interaction (E_k). Second, for near-neighbor pair-flips, the intrinsic nuclear interaction is much stronger than the hyperfine mediated one for the field strength under consideration. Third, for nonlocal pair-flips, the intrinsic interaction is negligible due to its finite-range characteristic. Thus we can separate the flip-pairs into one subset, $k \in K_A$, which contains $O(N^2)$ nonlocal flip-pairs, driven by the effective pseudomagnetic field $\mathbf{h}^{\pm}_k \approx (\pm 2A_k, 0, \pm E_k)$ and a second subset, $k \in K_B$, which contains $O(N)$ near-neighbor flip-pairs, driven by $\mathbf{h}^{\pm}_k \approx (2B_k, 0, \pm E_k)$. The conjugate pseudospins will precess along opposite directions in the nonlocal subset K_A, and symmetrically with respect to the y-z plane in the near-neighbor subset K_B. The decoherence can be readily grouped by the two different mechanisms as

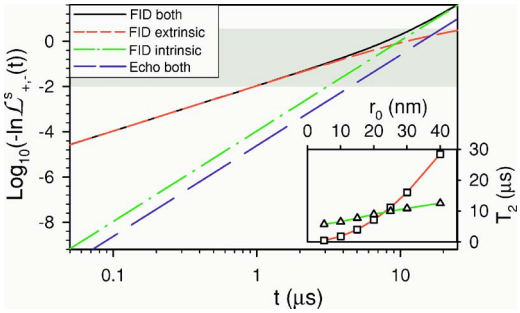

FIG. 2. (Color online) Separated contributions to the single-system FID by the extrinsic hyperfine-mediated nuclear coupling, the intrinsic nuclear interaction, and both, for a dot with $L_{[001]}$ =6.2 nm and r_0=25 nm at B_{ext}=12 T. The spin-echo profile with both mechanisms is shown in comparison. The inset shows the FID decoherence times resulting from only the hyperfine-mediated interaction (square symbol) or only the intrinsic interaction (triangle symbol) as functions of r_0.

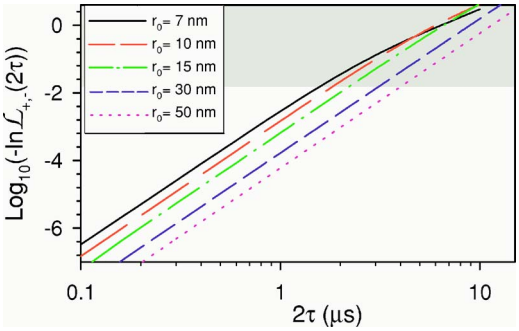

FIG. 3. (Color online) Spin-echo signal for dots of $L_{[001]}=2.8$ nm and various r_0 at $B_{\text{ext}}=10$ T.

$$\mathcal{L}^{s}_{+,-} \cong \prod_{k\in K_B} e^{-(t^4/2)E_k^2B_k^2\,\text{sinc}^4(h_kt/2)} \prod_{k\in K_A} e^{-2t^2A_k^2\,\text{sinc}^2(h_kt)}, \tag{16}$$

where $h_k=|\mathbf{h}_k^{\pm}|$ and $\text{sinc}(x)\equiv\sin(x)/x$. We can see that the extrinsic hyperfine-mediated and the intrinsic couplings lead to the $e^{-(t/T_{2,A})^2}$ and the $e^{-(t/T_{2,B})^4}$ behavior in time shorter than the inverse pair-flip energy cost (which corresponds to the width of the excitation spectrum),

$$T_{2,B}\approx b^{-1/2}\mathcal{A}^{-1/2}N^{1/4}, \quad T_{2,A}\approx\Omega_e\mathcal{A}^{-2}N, \tag{17}$$

where b is the typical value of near-neighbor intrinsic nuclear coupling strength B_k and $\mathcal{A}\equiv\Sigma_n a_n$ is the hyperfine constant. Equation (17) explains the dot-size dependence of the two mechanisms in the inset of Fig. 2. When the two mechanisms are comparable, the single-system FID begins with e^{-t^2} behavior and may cross over towards e^{-t^4} decay as time increases, and this is actually observed in Fig. 2. As the time grows beyond the inverse excitation spectrum width, the quantum kinetics becomes a stochastic Markovian process by building up the energy-conserving Fermi-Golden rule as indicated by the sinc function in Eq. (16).

Figure 3 shows the onset of the Markovian process by the crossover from the e^{-t^4} short-time behavior to the long-time exponential decay e^{-t}.

In ensemble or repeated dynamics,[17,18,20] FID will be dominated by the inhomogeneous broadening. In ESR experiments,[36,37] electron spin-flip pulses can be applied to eliminate the effects of the static fluctuations of the local field and spin-echo profiles are measured. The echo decay time T_H (defined as the echo delay time at which the spin-echo magnitude drops to $1/e$ of the zero delay value) is generally believed to give a quantitative measure of the single-system FID time T_2, as the direct measurement of the latter is of considerable difficulty with current experimental capability. We now show that the echo pulse will also modify the electron spin decoherence induced by the quantum pair-flip dynamics, and as a consequence, T_H and T_2 can be significantly different. As the electron spin is reversed by the π pulse, the hyperfine-mediated transition amplitude A_k and the hyperfine energy cost E_k for each pair-flip will change the sign after the pulse. Thus, the pseudospins driven by the extrinsic hyperfine-mediated nuclear coupling (in subset K_A)

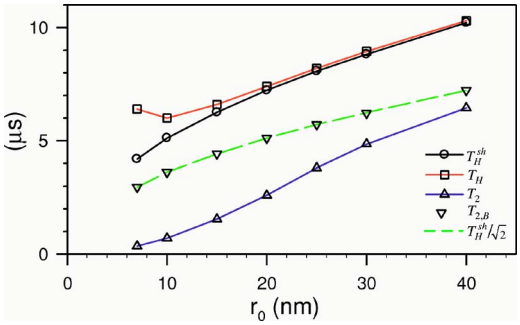

FIG. 4. (Color online) Dot-size dependence of the decoherence times (see text), T_H^{sh} as circles, T_H squares, T_2 triangles, $T_{2,B}$ inverted triangles. $T_H^{\text{sh}}/\sqrt{2}$ is plotted (dashed blue line) for compare with $T_{2,B}$. The dot thickness $L_{[001]}=2.8$ nm and $B_{\text{ext}}=10$ T.

will reverse their precession after the pulse and return to the origin at $t=2\tau$, disentangling the electron spin and the pseudospins. So the decoherence driven by the extrinsic hyperfine-mediated coupling is largely eliminated in the spin-echo configuration (see Fig. 2). This phenomenon was first noted in the numerical simulation of a small system of $\sim$10 nuclear spins in Ref. 5. For the pseudospin driven by the intrinsic coupling (subset K_B), the conjugate pseudospins will switch their precession axis which also reverse the entanglement to some extent but no full recovery can be obtained at the echo time. Finally, the electron spin coherence at the echo time can be derived as

$$\mathcal{L}_{+,-}(2\tau) \cong \prod_{k\in K_B} e^{-2\tau^4E_k^2B_k^2\,\text{sinc}^4(h_k^B\tau/2)}. \tag{18}$$

Similar to the analysis for single system FID, the spin-echo signal begins with $e^{-(2\tau/T_H^{\text{sh}})^4}$ short-time behavior. The Fermi-Golden rule will build up as the time grows beyond the inverse pair-excitation spectrum width, which renders the quantum kinetics a Markovian process. The crossover towards the Markovian behavior becomes observable when the width of the pair-excitation spectrum is greater than or comparable to the inverse of the initial dephasing time T_H^{sh}. For small quantum dots, the hyperfine coupling and its gradient is larger, resulting in a broader excitation spectrum, and therefore the crossover behavior is observable, as shown in Fig. 3. For large quantum dots, where the pair-excitation spectrum is relatively narrower, the initial stage decay could already eliminate the spin coherence and thus the whole dephasing process could be described by the $e^{-(2\tau/T_H^{\text{sh}})^4}$ profile.

The decoherence due to the intrinsic nuclear interaction is suppressed by the echo pulse as evidenced by the enhancement of the short-time decoherence time, $T_H^{\text{sh}}=\sqrt{2}T_{2,B}$ (see Figs. 2 and 4). The onset of the Markovian crossover also manifests itself in the difference between the initial echo time T_H^{sh} and the overall echo decay time T_H for small dots, as shown in Fig. 4.

VI. SUMMARY

In conclusion, we have presented the quantum theory for the electron spin decoherence by a bath of interacting nuclear

spins under strong magnetic field and at finite temperature. Entanglement between electron and nuclear spins, established by their coupled evolution, leads to the loss of electron spin coherence. The solution to the electron spin coherence amounts to solving the many-body dynamics of the interacting nuclear spin bath, which are conditioned on different electron spin states. In the time scale of interest, the nuclear bath dynamics is dominated by pair correlations among nuclear spins, which can be mapped into independent pseudospin excitations. Within the pair-correlation approximation, the electron-nuclear spin dynamics reduces to the coupled evolution of the electron spin with the noninteracting pseudospin excitations, for which exact solutions are found.

Decoherence behaviors in GaAs quantum dots are calculated as examples. We have demonstrated the significance of the extrinsic nuclear coupling mediated by the virtual electron spin flips, which manifests itself in the strong field dependence of the FID in single-system dynamics. The calculated electron spin decoherence time in single-system FID varies from $\sim 0.1\ \mu$s to $\sim 10\ \mu$s for field strength from 1 T to 20 T, and saturates as the hyperfine mediated coupling is suppressed by stronger field. The spin-echo pulse not only recovers the coherence lost by inhomogeneous broadening but also eliminates the decoherence due to the hyperfine-mediated nuclear pair-flips and reduces the decoherence by the intrinsic nuclear interaction, leading to a spin-echo decay time $\sim 10\ \mu$s independent of field strength in ensemble dynamics.

The theory presented here can be applied to other electron-nuclear spin systems, e.g., donor impurities in silicon, and may also be extended to even more general cases of a quantum object in contact with an interacting bath.

ACKNOWLEDGMENTS

This work was supported by NSF Grant No. DMR-0403465, ARO/LPS, and DARPA/AFOSR.

APPENDIX A: THE HAMILTONIAN

The total Hamiltonian of the system of an electron and many nuclear spins is given by

$$\hat{H} = \hat{H}_e + \hat{H}_N + \hat{H}_{eN} + \hat{H}_{NN}, \tag{A1}$$

composed of the single spin Zeeman energies $\hat{H}_e = \Omega_e \hat{S}_e^z$ and $\hat{H}_N = \Sigma_n \omega_n \hat{J}_n^z$ in the applied magnetic field along the z axis, the hyperfine interaction $\hat{H}_{eN}$ and the intrinsic nuclear-nuclear interaction $\hat{H}_{NN}$.

The hyperfine interaction between the electron and the nuclear spins consists of the isotropic Fermi contact interaction and the anisotropic dipole-dipole interaction. The latter is negligible since the electron wave function in a quantum dot is dominated by the s-orbit states. The contact hyperfine interaction is given by[38]

$$\hat{H}_{eN} = \sum_n a_n \hat{\mathbf{S}}_e \cdot \hat{\mathbf{J}}_n, \tag{A2a}$$

$$a_n = \frac{\mu_0}{4\pi} \gamma_e \gamma_n \frac{8\pi}{3} |\Psi(\mathbf{R}_n)|^2, \tag{A2b}$$

where μ_0 is the vacuum magnetic permeability, $\mathbf{R}_n$ denotes the coordinates of the nth nucleus, γ_n is the nuclear gyromagnetic ratio, and γ_e is the electron gyromagnetic ratio. It should be noted that while the effective g factor in the quantum dot determines the Zeeman energy Ω_e, the free electron g factor +2.0023 should be used for the hyperfine coupling.[39]

The intrinsic interaction between nuclear spins includes the direct dipole-dipole interaction, the indirect interactions mediated by virtual excitation of electron-hole pairs, and the intranuclear quadrupole interaction. The direct dipole term is given by[38]

$$\hat{H}_{NN}^d = \sum_{n<m} \frac{\mu_0}{4\pi} \frac{\gamma_n \gamma_m}{R_{n;m}^3} \left(\hat{\mathbf{J}}_n \cdot \hat{\mathbf{J}}_m - \frac{3 \hat{\mathbf{J}}_n \cdot \mathbf{R}_{n;m} \mathbf{R}_{n;m} \cdot \hat{\mathbf{J}}_m}{R_{n;m}^2} \right), \tag{A3}$$

with $\mathbf{R}_{n;m} \equiv \mathbf{R}_n - \mathbf{R}_m$. The indirect nuclear interaction is mediated via the virtual excitation of electron-hole pairs by the hyperfine interaction between nuclei and valence electrons.[23–27] When the virtual excitation is caused by the Fermi-contact hyperfine interaction, the indirect interaction has the isotropic exchange form

$$\hat{H}_{NN}^{\mathrm{ex}} = -\sum_{n<m} B_{n;m}^{\mathrm{ex}} \hat{\mathbf{J}}_n \cdot \hat{\mathbf{J}}_m, \tag{A4}$$

named the pseudoexchange interaction in the literature. The leading contribution of the pseudoexchange interaction for nearest neighbors in the host crystal can be expressed as[24,25]

$$B_{n;m}^{\mathrm{ex}} = \frac{\mu_0}{4\pi} \frac{\gamma_n^{\mathrm{ex}} \gamma_m^{\mathrm{ex}}}{R_{n;m}^3} \frac{a_0}{R_{n;m}}, \tag{A5}$$

where γ_n^{ex} is the effective gyromagnetic ratio determined by the renormalized charge density of the s-orbit electron. The indirect exchange interaction has been experimentally studied by many researchers.[25–27]

When the virtual excitation of electron-hole pairs involves both the Fermi contact and the dipolar hyperfine interactions, group theoretical analysis shows that the indirect nuclear spin interaction has the dipolar form and is denoted as indirect pseudodipolar interaction in the literature.[23] Lattice distortion can result in local electric field gradients, inducing the intranuclear quadrupole interaction for nuclear spins with moment greater than 1/2. The indirect pseudodipolar interaction and the quadrupole interaction are not included in the numerical calculation in this paper due to the lack of experimental characterizations in the literature. Nonetheless, they can be well incorporated in our theory as contributions to energy cost and transition amplitude for nuclear pair-flips [see Eqs. (C2b) and (C2c)] when reliable data is available. Furthermore, available studies[25–27] show that the direct dipolar interaction together with indirect exchange interaction can mainly account for the broadening and line shapes of NMR and NAR signals in the semiconductor matrix of our interest and thus shall be the main ingredients of the intrinsic nuclear interactions.

APPENDIX B: THE EXTRINSIC HYPERFINE-MEDIATED NUCLEAR SPIN-SPIN INTERACTION

The contact hyperfine interaction can be separated into the longitudinal (or diagonal) part

$$\hat{H}_{eN,l} \equiv \sum_n a_n \hat{S}_e^z \hat{J}_n^z, \tag{B1}$$

and the transverse (or off-diagonal) part

$$\hat{H}_{eN,t} \equiv \sum_n \frac{a_n}{2} (\hat{S}_e^+ \hat{J}_n^- + \hat{S}_e^- \hat{J}_n^+). \tag{B2}$$

The off-diagonal hyperfine interaction in the lowest order is eliminated by the standard canonical transformation,

$$\hat{W} \equiv \exp\left(\sum_n \frac{a_n}{2(\Omega_e - \omega_n)} (\hat{S}_e^+ \hat{J}_n^- - \hat{S}_e^- \hat{J}_n^+) \right). \tag{B3}$$

The residual second order term in the transformed Hamiltonian $\hat{H}_{\rm red} = \hat{W}\hat{H}\hat{W}^{-1}$ is $\hat{H}_A$ in Eq. (3a). We neglect higher order terms whose effects are by at least a factor of $\sim(\Omega_e\sqrt{N}/\mathcal{A})^{-2} \ll 1$ smaller as compared to $\hat{H}_A$. Note that while the Zeeman energy $\Omega_e \sim 10-100\ \mu$eV for field $\sim 1-10$ T,[17] $\mathcal{A}/\sqrt{N} \sim T_2^{*-1} \sim 0.1\ \mu$eV in GaAs fluctuation dots.[18]

The canonical transformation also rotates the basis states, $|\pm\rangle \otimes |\mathcal{J}\rangle$, $|\mathcal{J}\rangle \equiv \otimes_n |j_n\rangle$, by a small amount

$$\hat{W}|\pm\rangle \otimes |\mathcal{J}\rangle \approx \left(1 - \frac{1}{2}\sum_n |w_n^{\pm}|^2\right)|\pm\rangle \otimes |\mathcal{J}\rangle \mp \sum_n w_n^{\pm} |\mp\rangle \otimes |j_n \pm 1\rangle \underset{m\neq n}{\otimes} |j_m\rangle, \tag{B4}$$

where we have kept only the lowest order correction in terms of the expansion coefficient

$$w_n^{\pm} \equiv \frac{a_n}{2(\Omega_e - \omega_n)} \sqrt{j(j+1) - j_n(j_n \pm 1)}, \tag{B5}$$

which is small number due to the inequalities, $\Omega_e \gg \omega_n \gg a_n$. $j=3/2$ for all three relevant isotopes ^{75}As, ^{69}Ga, and ^{71}Ga.

The rotation of the state vector actually accounts for the rapid initial drop of the electron spin coherence. We show below that this reduction in the visibility of the spin beat is negligible under the field strength $\gtrsim 1$ T. The state evolution in the very initial stage ($t \lesssim a_n^{-1}$) can be expressed as

$$\begin{aligned} e^{-i\hat{H}t}|\pm\rangle \otimes |\mathcal{J}\rangle &= \hat{W}^{-1} e^{-i\hat{H}_{\rm red} t} \hat{W} |\pm\rangle \otimes |\mathcal{J}\rangle \\ &\approx \hat{W}^{-1} e^{-i(\hat{H}_e + \hat{H}_N + \hat{H}_{eN,l})t} \hat{W} |\pm\rangle \otimes |\mathcal{J}\rangle \\ &\approx e^{\mp i(1/2)(\Omega_e + \mathcal{E}_{\mathcal{J}})t} e^{-i\Sigma_n j_n \omega_n t} \\ &\times \left[\left(1 - \sum_n (1 - e^{\pm i(\Omega_e + \mathcal{E}_{\mathcal{J}} - \omega_n \pm a_n)t}) |w_n^{\pm}|^2 \right) \right. \\ &\times |\pm\rangle \otimes |\mathcal{J}\rangle \pm \sum_n (1 - e^{\pm i(\Omega_e + \mathcal{E}_{\mathcal{J}} - \omega_n \pm a_n)t}) \\ &\left. \times w_n^{\pm} |\mp\rangle \otimes |j_n \pm 1\rangle \underset{m\neq n}{\otimes} |j_m\rangle \right], \end{aligned} \tag{B6}$$

where $\mathcal{E}_{\mathcal{J}} = \Sigma_n j_n a_n$ is the Overhauser energy of the electron spin under the nuclear configuration $|\mathcal{J}\rangle$ which arises from the longitudinal (or diagonal) hyperfine interaction. To single out the process of visibility loss, we have omitted above the nuclear-nuclear coupling terms in $\hat{H}_{\rm red}$.[2] The reduced density matrix of the electron spin can be derived as

$$\rho_{+,+}^e(t) \approx \rho_{+,+}^e(0)[1 - p_+(t)] + \rho_{-,-}^e(0) p_-(t), \tag{B7a}$$

$$|\rho_{+,-}^e(t)| \approx |\rho_{+,-}^e(0)| \left(1 - \frac{p_+(t)}{2} - \frac{p_-(t)}{2}\right), \tag{B7b}$$

with

$$p_{\pm}(t) \equiv 4 \sum_n (w_n^{\pm})^2 \sin^2 \frac{(\Omega_e + \mathcal{E}_{\mathcal{J}} - \omega_n \pm a_n)t}{2}. \tag{B8}$$

The interference between different frequency components on the right-hand side (RHS) of Eq. (B8) will lead to a visibility loss of the coherence and the initial drop of the population with amplitude $\sim p_{\pm} \lesssim (\Omega_e\sqrt{N}/\mathcal{A})^{-2} \ll 1$, occurring in the time scale $\sim a_n^{-1}$. Therefore, in the high field limit ($\gtrsim 1$ T), the electron spin-flip by the nuclear spins is efficiently suppressed ($T_1 \to \infty$ if phonon mechanisms excluded).

To conclude, the transverse (or off-diagonal) part of the hyperfine interaction has two effects: (i) the transformation acting on the Hamiltonian results in an effective coupling between the nuclear spins [$\hat{H}_A$ in Eq. (3)], which contribute to the pure dephasing of the electron spin coherence; (ii) the transformation acting on the state vector can be understood as a visibility loss. While the two processes coexist, we have shown that under the field strength $\gtrsim 1$ T, the visibility loss is negligibly small. Therefore, the exact evolution of the electron nuclear system can be well approximated as

$$e^{-i\hat{H}t}|\pm\rangle \otimes |\mathcal{J}\rangle \cong e^{-i\hat{H}_{\rm red} t}|\pm\rangle \otimes |\mathcal{J}\rangle \tag{B9}$$

with the effect of the transverse hyperfine interaction well incorporated as the extrinsic nuclear coupling $\hat{H}_A$.

APPENDIX C: SOLUTION OF THE DYNAMICS OF THE ELECTRON-NUCLEAR SPIN SYSTEM

The elementary process driven by the interaction Hamiltonian, Eq. (2), is the pairwise homonuclear spin flip-flop. Here, we examine the dynamics of the basic flip-flop process, based on which we build a hierarchical framework of many-spin basis states for dynamics, investigate the spin correlations, and construct a pseudospin method.

1. The basic nuclear spin excitation

The transition for the pair-flip driven by the operator $\hat{J}_n^+ \hat{J}_m^-$ consists in a pair of nuclear spins in state $|j_n, j_m\rangle$ going to $|j_n+1, j_m-1\rangle$ if permitted, i.e., $j_n + 1 \leqslant j$ and $j_m - 1 \geqslant -j$ for spin j. The shorthand k is used to denote this pair transition. Such a kth pair-flip transition between two many-nuclear spin states is described as

$$|\pm\rangle|\mathcal{J}\rangle \to |\pm\rangle|\mathcal{J},k\rangle. \tag{C1}$$

The transition matrix element $\pm A_k + B_k$ and the energy cost $D_k \pm E_k$, the sign conditioned on the electron spin state $|\pm\rangle$, can be derived from Eq. (3),

$$A_k \equiv \langle \mathcal{J},k|\hat{H}_A|\mathcal{J}\rangle = \frac{a_n a_m}{4\Omega_e}\sqrt{j(j+1)-j_n(j_n+1)}\sqrt{j(j+1)-j_m(j_m-1)}, \tag{C2a}$$

$$B_k \equiv \langle \mathcal{J},k|\hat{H}_B|\mathcal{J}\rangle = B_{n,m}\sqrt{j(j+1)-j_n(j_n+1)}\sqrt{j(j+1)-j_m(j_m-1)}, \tag{C2b}$$

$$D_k \equiv \langle \mathcal{J},k|\hat{H}_D|\mathcal{J},k\rangle - \langle \mathcal{J}|\hat{H}_D|\mathcal{J}\rangle = \sum_{n'} D_{n,n'} j_{n'} - \sum_{m'} D_{m,m'} j_{m'} - D_{n,m}, \tag{C2c}$$

$$E_k \equiv \langle \mathcal{J},k|\hat{H}_E|\mathcal{J},k\rangle - \langle \mathcal{J}|\hat{H}_E|\mathcal{J}\rangle = (a_n - a_m)/2. \tag{C2d}$$

2. The hierarchy of nuclear pair-flip states

The evolution of the nuclear spin state $|\mathcal{J}^{\pm}(t)\rangle \equiv e^{-i\hat{H}^{\pm}t}|\mathcal{J}\rangle$ can be formally described by pair-flip transitions in a hierarchy of basis states. The hierarchy is composed of the seed state, $|\mathcal{J}\rangle$, the first-generation states, each $|\mathcal{J},k\rangle$ generated from the seed state by the kth pair-flip, the second-generation states, each $|\mathcal{J},k_1,k_2\rangle$ generated from the first-generation state $|\mathcal{J},k_1\rangle$ or $|\mathcal{J},k_2\rangle$ by the k_2th or the k_1th pair-flip, respectively, and so on. A many-nuclear spin state can be expanded in this basis as

$$|\mathcal{J}^{\pm}(t)\rangle = C^{\pm}_{\mathcal{J}}(t)|\mathcal{J}\rangle + \sum_{k_1} C^{\pm}_{\mathcal{J},k_1}(t)|\mathcal{J},k_1\rangle + \sum_{k_1,k_2} C^{\pm}_{\mathcal{J},k_1,k_2}(t) \times |\mathcal{J},k_1,k_2\rangle + \cdots, \tag{C3}$$

in which the wave function satisfies the equation

$$\partial_t C^{\pm}_{\mathcal{J},k_1,\ldots,k_p} = -iE^{\pm}_{\mathcal{J},k_1,\ldots,k_p} C^{\pm}_{\mathcal{J},k_1,\ldots,k_p} - i\sum_{j=1}^{p}\sum_{k_j} (B_{k_j} \pm A_{k_j}) C^{\pm}_{\mathcal{J},k_1,\ldots,k_{j-1},k_{j+1},\ldots,k_p} - i\sum_{k\neq k_1,\ldots,k_p} (B^*_k \pm A^*_k) C^{\pm}_{\mathcal{J},k_1,\ldots,k_p,k}, \tag{C4}$$

where the energy $E^{\pm}_{\mathcal{J},k_1,\ldots,k_p}$ is the eigenenergy of the basis state $|\mathcal{J},k_1,\ldots,k_p\rangle$ under the Hamiltonian $\hat{H}_D \pm \hat{H}_E$, respectively. The hierarchy description of the nuclear spin dynamics is illustrated in Fig. 5.

The many-body nature of the problem lies in the fact that the pairwise flip-flops are correlated in general. The correlation between two pair-flips can be developed in the following three cases:

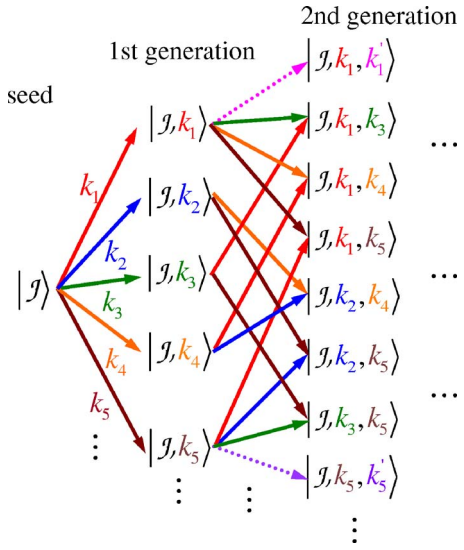

FIG. 5. (Color online). The hierarchy structure for the nuclear spin state evolution driven by pairwise flip-flops. The k_1' and k_5' pair-flips are possible only when the pair-flips k_1 and k_5 have taken place, respectively. Some pair-flips occurs exclusively to each other, such as k_2 and k_3.

(1) *Exclusive pair-flips* as shown in Figs. 6(a) and 6(b). When one pair-flip (k_1) has taken place, the other one (k_2) which shares one or two spins with the flipped pair cannot occur any more, and vice versa.

(2) *Subsequent pair-flips* as shown in Figs. 6(c) and 6(d). When two pair-flips share one or two nuclear spins, one pair-flip is possible only after the other one has already taken place.

(3) *Neighboring pairs* as shown in Fig. 6(e). Two pair-flips can be correlated even when they do not share a nuclear spin but are in the neighborhood, since one pair-flip will change the nuclear spin configuration in the neighborhood of the other pair and thus modify the energy cost (D_k) due to the

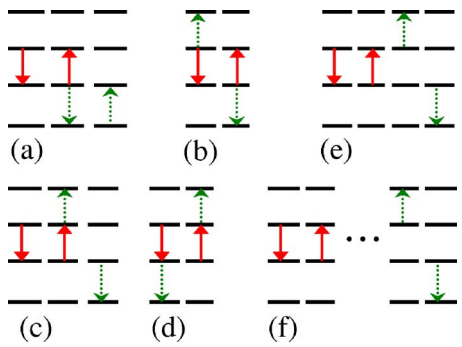

FIG. 6. (Color online) Possible correlations between two nuclear spin pair-flips (k_1 and k_2, indicated by solid and dotted arrows, respectively). (a) and (b), the two pair-flips sharing one or two nuclei occur exclusively to each other. (c) and (d), one pair-flip can take place only after the other pair has been flipped. (e) The energy cost D_k of one pair-flip depends on whether or not the other pair has been flipped, when they involve spins in the neighborhood. (f) The two pair-flips are independent of each other when they are far apart from each other.

diagonal nuclear spin interactions of one pair-flip. This correlation can be clearly seen from Eq. (C2c).

When two pairwise flip-flops are not in the neighborhood [Fig. 6(f)], they are independent of each other.

With increasing numbers of pair-flips, the nuclear spin state involves basis states further up in the hierarchy structure depicted in Fig. 5, and higher order correlations may occur, making the solution of nuclear spin dynamics a formidable task in general.

3. Pair-correlation approximation (PCA)

Two pair-flips are correlated only when they are located in the neighborhood. We can estimate the probability of having pair-flips correlated in the pth generation of the hierarchy: if $p-1$ pair-flip excitations have been generated, the probability of having the pth pair outside the neighborhood of all the previous ones is about $[1-q(p-1)/N]$. By induction, the probability of having p pair-flips uncorrelated is

$$1 - P_{\mathrm{corr}} \sim \prod_{j=1}^{p-1} (1 - qj/N) \sim \exp(-qp^2/N). \tag{C5}$$

The number of pair-flip excitations at time t may be estimated by

$$N_{\mathrm{flip}} \equiv \max_{\mu=\pm} \left(\sum_{p=1}^{\infty} p \left| C^{\mu}_{J,k_1,\ldots,k_p} \right|^2 \right). \tag{C6}$$

If $qN^2_{\mathrm{flip}}(t) \ll N$ in the time scale of interest, the probability, P_{corr}, of having pair-flip excitations correlated is negligibly small. Thus, by removing the few states reached via subsequently correlated pair-flips and adding few states containing exclusive pair-flips, the exact Hilbert space can be mapped into the tensor product of two-dimensional Hilbert subspaces, each of them corresponding to a pair-flip available from the seed state $|\mathcal{J}\rangle$, namely

$$\{|\mathcal{J}\rangle, |\mathcal{J},k_1\rangle, |\mathcal{J},k_1,k_2\rangle, \ldots\} \rightarrow \bigotimes_k \{|\uparrow_k\rangle, |\downarrow_k\rangle\}, \tag{C7}$$

where the index k runs over all possible pair-flips from the seed state to the first generation. The mapping can be explicitly expressed as

$$|\mathcal{J}\rangle \rightarrow \bigotimes_k |\uparrow_k\rangle, \tag{C8a}$$

$$|\mathcal{J},k_1\rangle \rightarrow |\downarrow_{k_1}\rangle \bigotimes_{k\neq k_1} |\uparrow_k\rangle, \tag{C8b}$$

$$|\mathcal{J},k_1,k_2\rangle \rightarrow |\downarrow_{k_1}\rangle |\downarrow_{k_2}\rangle \bigotimes_{k\neq k_1,k_2} |\uparrow_k\rangle, \tag{C8c}$$

etc., and the nuclear bath state can be factorized into elementary excitations as

$$|\mathcal{J}^{\pm}(t)\rangle = e^{-iE^{\pm}_{\mathcal{J}}t} \bigotimes_k [g^{\pm}_k(t)|\uparrow_k\rangle + f^{\pm}_k(t)|\downarrow_k\rangle]. \tag{C9}$$

Furthermore, the energy cost of a pair-flip is assumed independent of whether or not another pair-flip has occurred in the neighborhood. So all the elementary excitations are treated independent of each other and their dynamics is determined solely by their own energy costs and transition matrix elements as

$$i\partial_t g^{\pm}_k = (B_k \pm A_k) f^{\pm}_k, \tag{C10a}$$

$$i\partial_t f^{\pm}_k = (D_k \pm E_k) f^{\pm}_k + (B_k \pm A_k) g^{\pm}_k, \tag{C10b}$$

with initial conditions $g^{\pm}_k(0)=1$ and $f^{\pm}_k(0)=0$. The above approximation strategy is denoted as the pair-correlation approximation (PCA) where all pair-correlations among the nuclear spins are kept and higher order nuclear correlations are neglected.

In PCA, we will calculate physical properties by using Eq. (C9) as the bath state at time t instead of the exact state Eq. (C4). In this paper, the electron spin coherence of interest is essentially the state overlap between two differently driven bath state as shown in Eq. (12a). The relative amount of change to the bath Hilbert space structure by PCA is P_{corr}. Therefore, the relative error of PCA in calculating the coherence is bounded by

$$\epsilon \lesssim P_{\mathrm{corr}} \sim 1 - \exp(-qN^2_{\mathrm{flip}}/N). \tag{C11}$$

4. The pseudospin model

The uncorrelated pair-flip dynamics given in Eq. (C10) is nothing but the independent evolutions of two-level systems $\{|\uparrow_k\rangle, |\downarrow_k\rangle\}$. Thus the electron-nuclear spin dynamics $|\mathcal{J}^{\pm}(t)\rangle$ from the initial state $|\mathcal{J}\rangle$ is mapped, by PCA, to the precession of $\mathcal{N}$ noninteracting pseudospins under pseudofields conditioned on the electron spin state

$$\hat{\mathcal{H}}^{\pm}_k \equiv \mathbf{h}^{\pm}_k \cdot \hat{\boldsymbol{\sigma}}_k/2, \tag{C12a}$$

$$\mathbf{h}^{\pm}_k \equiv (\pm 2A_k + 2B_k, 0, D_k \pm E_k), \tag{C12b}$$

where $\hat{\boldsymbol{\sigma}}_k \equiv (\hat{\sigma}^x_k, \hat{\sigma}^y_k, \hat{\sigma}^z_k)$ is the Pauli matrix for the pseudospin corresponding to the kth pairflip available from the seed state $|\mathcal{J}\rangle$. Note that by the Hamiltonian mapping from Eq. (2) to Eq. (13), the energy of the seed state has been shifted by a constant $\Sigma_k(D_k \pm E_k)/2$, which does not affect the calculation of $|\langle \mathcal{J}^-(t)|\mathcal{J}^+(t)\rangle|$. The directions (indicated by the superscripts x, y, and z) for the pseudospins are not defined in the real-space but in a fictitious pseudospace.

APPENDIX D: RANGE OF VALIDITY OF THE PAIR-CORRELATION APPROXIMATION

Within the PCA, the averaged pair-flip number N_{flip} defined in Eq. (C6) has a simpler form

$$N_{\mathrm{flip}} = \max_{\pm} \left(\sum_k |\langle\uparrow|e^{-i\mathcal{H}^{\pm}_k t}|\uparrow\rangle|^2 \right), \tag{D1}$$

with which we can make an *a posterior* self-consistency check of the validity of the approximation. If N_{flip} obtained from Eq. (D1) is small, we conclude that it also faithfully reflects the number of pair-flip excitations in the exact dynamics and therefore, the error estimation would be faithful

and the physical property can be calculated based on PCA with a relative error bounded by Eq. (C11).

The total number of pair-flip excitations can be divide into two parts: $N_{\mathrm{flip}}(t)=N_{\mathrm{flip},A}(t)+N_{\mathrm{flip},B}(t)$, where $N_{\mathrm{flip},A}$ is the number of nonlocal pair-flip excitations and $N_{\mathrm{flip},B}$ is the number of local pair-flip excitations that have been created. $N_{\mathrm{flip},A}(t)$ and $N_{\mathrm{flip},B}(t)$ have very different dependence on time and system parameters, and we analyze them separately.

In free-induction evolution, the number of nonlocal pair-flip excitations is given by

$$N_{\mathrm{flip},A}(t)=\sum_k\left(\frac{2A_k}{\sqrt{E_k^2+4A_k^2}}\right)^2\sin^2\frac{\sqrt{E_k^2+4A_k^2}t}{2}$$
$$\leqslant\sum_k A_k^2t^2\sim\mathcal{N}_A\frac{\mathcal{A}^4}{N^4\Omega_e^2}t^2\sim\frac{\mathcal{A}^4}{N^2\Omega_e^2}t^2, \qquad \text{(D2)}$$

where $\mathcal{N}_A\sim N^2$ is the number of nonlocal nuclear spin pairs. Since the evolution of the nonlocal pair correlation is completely reversed by the π pulses (see the discussion in Sec. V), $N_{\mathrm{flip},A}(t)$ is also reversed and returns to zero at each spin-echo time. Therefore, $N_{\mathrm{flip},A}(t)$ does not accumulate in the pulse controlled dynamics[22] and we just need to look at the maximum value of $N_{\mathrm{flip},A}(t)$ between echoes.

For single system FID and ensemble spin-echo calculation presented in this paper, the sufficient condition for PCA to be valid is $N_{\mathrm{flip},A}^2(T_H)\ll N$ by noticing that $T_2\approx\min(T_{2,A},T_{2,B})$ and $T_H=\sqrt{2}T_{2,B}$. From Eq. (17), we have,

$$N_{\mathrm{flip},A}(T_H)\sim N^{-3/2}\Omega_e^{-2}b^{-1}\mathcal{A}^3, \qquad \text{(D3)}$$

Therefore, we obtain a lower bound on the dot size N for the validity of PCA: $N^4\gg\mathcal{A}^6\Omega_e^{-4}b^{-2}$. For GaAs fluctuation dot in a field of 10 T, the above condition is well satisfied for $N\gtrsim10^4$.

In contrast to the nonlocal pair dynamics, the local pair dynamics is *not* reversed under the influence of the electron spin-flip and $N_{\mathrm{flip},B}(t)$ accumulates all through the time. Nonetheless, it turns out that for all scenarios of interest including the evolution under the pulse sequence control as in Ref. 22, we have,

$$N_{\mathrm{flip},B}(t)\leqslant\sum_k B_k^2t^2\sim\mathcal{N}_Bb^2t^2\sim Nb^2t^2, \qquad \text{(D4)}$$

where $\mathcal{N}_B\sim N$ is the number of local nuclear spin pairs. For the relevance of the single system FID and ensemble spin-echo calculation, we shall examine

$$N_{\mathrm{flip},B}(T_H)\sim N^{3/2}b\mathcal{A}^{-1} \qquad \text{(D5)}$$

and therefore, the condition $(N_{\mathrm{flip},B})^2\ll N$ sets an upper bound on the quantum dot size N: $N^2b^2\mathcal{A}^{-2}\ll1$. In GaAs, the above condition is well satisfied for quantum dot size $N\lesssim10^8$.

To conclude, for nuclear pair correlations to dominate over higher order correlations in the relevant time scale, local nuclear pair dynamics driven by the intrinsic couplings imposes an upper bound on N while non local nuclear pair dynamics driven by the extrinsic coupling imposes a lower bound. This mesoscopic regime covers quantum dots of all practical size. Within this mesoscopic regime, higher order nuclear correlations are well negligible under the time scale of interest. The error estimation is based on characterizing the difference in the Hilbert space structure of the exact dynamics and that of the pseudospin model and assuming this difference has a full influence on the electron spin coherence calculation. Therefore, the bound of Eq. (C11) is not necessarily a tight bound.

*Present address: Department of Physics, The University of Texas, Austin, Texas 78712-0264, USA.

[1] P. W. Anderson, Phys. Rev. **114**, 1002 (1959).
[2] A. V. Khaetskii, D. Loss, and L. Glazman, Phys. Rev. Lett. **88**, 186802 (2002).
[3] I. A. Merkulov, A. L. Efros, and M. Rosen, Phys. Rev. B **65**, 205309 (2002).
[4] W. A. Coish and D. Loss, Phys. Rev. B **70**, 195340 (2004).
[5] N. Shenvi, R. de Sousa, and K. B. Whaley, Phys. Rev. B **71**, 224411 (2005).
[6] R. de Sousa and S. Das Sarma, Phys. Rev. B **68**, 115322 (2003).
[7] W. M. Witzel, R. de Sousa, and S. Das Sarma, Phys. Rev. B **72**, 161306(R) (2005).
[8] Y. G. Semenov and K. W. Kim, Phys. Rev. Lett. **92**, 026601 (2004).
[9] A. V. Khaetskii and Y. V. Nazarov, Phys. Rev. B **61**, 12639 (2000).
[10] L. M. Woods, T. L. Reinecke, and Y. Lyanda-Geller, Phys. Rev. B **66**, 161318(R) (2002).
[11] V. N. Golovach, A. Khaetskii, and D. Loss, Phys. Rev. Lett. **93**, 016601 (2004).
[12] C. Deng and X. Hu, Phys. Rev. B **73**, 241303(R) (2006).
[13] T. Fujisawa, D. G. Austing, Y. Tokura, Y. Hirayama, and S. Tarucha, Nature (London) **419**, 278 (2002).
[14] J. M. Elzerman, R. Hanson, L. H. Willems van Beveren, B. Witkamp, L. M. K. Vandersypen, and L. P. Kouwenhoven, Nature (London) **430**, 431 (2004).
[15] M. Kroutvar, Y. Ducommun, D. Heiss, M. Bichler, D. Schuh, D. Abstreiter, and J. J. Finley, Nature (London) **432**, 81 (2004).
[16] M. Atatüre, J. Dreiser, A. Badolato, A. Högele, K. Karrai, and Imamoglu, Science **312**, 551 (2006).
[17] M. V. Gurudev Dutt, J. Cheng, B. Li, X. Xu, X. Li, P. R. Berman, D. G. Steel, A. S. Bracker, D. Gammon, S. E. Economou, R. B. Liu, and L. J. Sham, Phys. Rev. Lett. **94**, 227403 (2005).
[18] A. S. Bracker, E. A. Stinaff, D. Gammon, M. E. Ware, J. G. Tischler, A. Shabaev, A. L. Efros, D. Park, D. Gershoni, V. L. Korenev, and I. A. Merkulov, Phys. Rev. Lett. **94**, 047402 (2005).
[19] F. H. L. Koppens, J. A. Folk, J. M. Elzerman, R. Hanson, L. H. W. van beveren, I. T. Vink, H. P. Tranitz, W. Wegscheider, L. P. Kouwenhoven, and L. M. K. Vandersypen, Science **309**, 1346 (2005).
[20] A. C. Johnson, J. R. Petta, J. M. Taylor, A. Yacoby, M. D. Lukin, C. M. Marcus, M. P. Hanson, and A. C. Gossard, Nature (Lon-

don) **435**, 925 (2005).
[21] N. V. Prokof'ev and P. C. E. Stamp, Rep. Prog. Phys. **63**, 669 (2000).
[22] Wang Yao, Ren-Bao Liu, and L. J. Sham, cond-mat/0604634 (unpublished).
[23] N. Bloembergen and T. J. Rowland, Phys. Rev. **97**, 1679 (1955).
[24] P. W. Anderson, Phys. Rev. **99**, 623 (1955).
[25] R. G. Shulman, J. M. Mays, and D. W. McCall, Phys. Rev. **100**, 692 (1955).
[26] R. G. Shulman, B. J. Wyluda, and H. J. Hrostrowski, Phys. Rev. **109**, 808 (1958).
[27] R. K. Sundfors, Phys. Rev. **185**, 458 (1969).
[28] W. Rhim, A. Pines, and J. Waugh, Phys. Rev. Lett. **25**, 218 (1970).
[29] S. Zhang, B. H. Meier, and R. R. Ernst, Phys. Rev. Lett. **69**, 2149 (1992).
[30] H. M. Pastawski, G. Usaj, P. R. Levstein, J. Raya, and J. Hirschinger, Physica A **283**, 166 (2000).
[31] R. Jalabert and H. M. Pastawski, Phys. Rev. Lett. **86**, 2490 (2001).
[32] F. M. Cucchietti, D. A. R. Dalvit, J. P. Paz, and W. H. Zurek, Phys. Rev. Lett. **91**, 210403 (2003).
[33] H. T. Quan, Z. Song, X. F. Liu, P. Zanardi, and C. P. Sun, Phys. Rev. Lett. **96**, 140604 (2006).
[34] D. Paget, G. Lampel, and B. Sapoval, Phys. Rev. B **15**, 5780 (1977).
[35] E. L. Hahn, Phys. Rev. **80**, 580 (1950).
[36] A. M. Tyryshkin, S. A. Lyon, A. V. Astashkin, and A. M. Raitsimring, Phys. Rev. B **68**, 193207 (2003).
[37] E. Abe, K. M. Itoh, J. Isoya, and S. Yamasaki, Phys. Rev. B **70**, 033204 (2004).
[38] C. P. Slichter, *Principles of Magnetic Resonance*, 3rd ed. (Springer-Verlag, Berlin, 1992).
[39] Y. Yafet, J. Phys. Chem. Solids **21**, 99 (1961).